Mechanism of Ionic Conductivity in Poly(ethyleneglycol 400)/$(LiCl)_x$ Electrolytic Complexes: Studies Based on Electrical Spectroscopy

Vito Di Noto,* Michele Vittadello, and Sandra Lavina

Dipartimento di Chimica Inorganica, Metallorganica ed Analitica, Università di Padova, Via Loredan, 4 35131 Padova, Italy

Maurizio Fauri and Simone Biscazzo

Dipartimento di Ingegneria Elettrica, Università di Padova, Via Gradenigo, 6/a, 35131 Padova, Italy

Received: January 31, 2001

This report describes the preparation of nine solvent-free (PEG400)/$(LiCl)_x$ complexes ($0.00207 \leq x \leq 1.40665$), together with a detailed investigation of their mechanisms of ion motion, carried out by impedance spectroscopy in the range from 20 Hz to 1 MHz. An accurate analysis of the real and imaginary components of their conductivities indicated that a full characterization of the AC electrical response for (PEG400)/$(LiCl)_x$ complexes requires an equivalent circuit analysis for frequencies lower than 1 kHz and a correlated ionic motion analysis based on a universal power law (UPL) for frequencies higher than 1 kHz. Ion−ion interactions in the (PEG400)/$(LiCl)_x$ systems were investigated by studying the equivalent conductivity profiles of the materials as a function of salt concentration and temperature. Results revealed the presence of two conductivity regions in (PEG400)/$(LiCl)_x$ materials, i.e., region I, detected at $0.0720 \leq c^{1/2} \leq 0.6214$ $(mol/kg)^{1/2}$, and region II, at $c^{1/2} \geq 0.6214$ $(mol/kg)^{1/2}$. The conductivity mechanisms proposed in these two regions are regulated by two phenomena: intrachain hopping (intra-CH) of ions between coordination sites distributed along the polyethereal chains and interchain hopping (inter-CH) migration of ions. These events were demonstrated to depend on the segmental motion, the distribution of "free" Cl^- ions along the PEG chains, and the site relaxation rate. This latter process takes place when a Li^+ ion hops "successfully" between two distinct polyethereal coordination sites. Finally, these materials show a conductivity of ca. 3.7×10^{-5} Scm^{-1} at 25 °C.

1. Introduction

During the past two decades, polymer electrolytes have attracted great interest because of their usage in lithium batteries.[1,3] Indeed, the replacement of liquid electrolytes with nonaqueous thin films of polymer electrolytes offers several advantages to battery technology: (a) low manufacturing cost and improved performance; (b) economy of volume and mass; (c) structural and chemical stability; (d) low toxicity; and (e) dual function as an electrode separator.[1] The classic polymer electrolytes consist of organic macromolecules (usually in the form of polyethereal units) that are doped with inorganic lithium salts. In an attempt to increase the conductivity of these materials, new types of polymer electrolytes have been obtained by modifying classical polymer electrolytes[1−7] in various ways. It has been demonstrated that polymer electrolytes (PE) suitable for technical applications in batteries require a high degree of amorphous conducting phase.[1] In general, this phase, which is responsible for the high conductivity of solid PE, is obtained by introducing liquid PE systems in the bulk solid PE or by plasticizing the latter. Several investigators suggested that conductivity in this systems takes place through two distinct events.[8,10] The first is associated with the charge migration of ions between coordination sites in the host material, and the second can be attributed to an increase in conductivity produced by polymeric chain motions, the so-called "segmental motion". To understand the ionic motion in the disordered phase, Ratner et al.[9−12] developed a dynamic bond percolation theory, which explains the charge migration in the system in terms of the renewal of hopping probabilities. In a study of the applicability of this theory, Furukawa et al.[13] reported accurate measurements of complex conductivity spectra for polypropylene oxide PPO/$(LiClO_4)_x$ complexes. These authors discussed their results on the basis of a dynamic bond percolation theory and proposed that conductivity takes place through two phenomena.[13,14] The first of these, which is detected at high frequencies, is associated with dielectric relaxations due to the dipolar motions caused by the segmental and normal-mode dynamics of the polymer host, and the second, which is revealed at lower frequencies, is attributed to local ionic motions.

To study the conductivity mechanism of polymer electrolytes in depth, we prepared extremely anhydrous polymer electrolytes. These materials allowed us to carry out very accurate impedance spectroscopy measurements as a function of concentration, temperature, and composition. As the mobility of the polymer host is a determining factor in controlling interchain and intrachain hopping (inter-CH and intra-CH, respectively) between sites on the polymer chains,[15−17] we decided to use a polymer with a molecular weight below the entanglement limit.[15−18] We present a detailed conductivity study of the resulting (PEG400)/$(LiCl)_x$ systems ($0.00207 \leq x \leq 1.40665$). The structures of these PEs and the interactions between the Li^+ and Cl^- ions and the poly(ethylene glycol) ligand were clearly elucidated by mid and far FT-IR spectroscopy.[19] Indeed,

* Author to whom correspondence should be addressed. E-mail: dinoto@ux1.unipd.it.

10.1021/jp0103934 CCC: $20.00
Published on Web 05/01/2001

in these PEs, it was demonstrated that: (a) the PEG chains assume a TGT type conformation; (b) Li^+ ions are preferentially coordinated by ethereal oxygens of the PEG ligand; (c) at an Li/O molar ratio of less than 0.036, Cl^- ions form hydrogen-bonding cages with the terminal OH groups of PEG chains; and (d) at an Li/O molar ratio greater than 0.036, Cl^- ions are present both in hydrogen bonds and as "free anions" along the PEG chains. All of these properties make the investigated materials particularly interesting to study by electrical spectroscopy. Indeed, it is reasonable to consider these systems as simple macromolecular liquids consisting of PEG400 rods with the coordination sites for cations located in a linear one-dimensional array along the chain axis.

In the present study, accurate electrical spectroscopic measurements were carried out in order to elucidate the conductivity mechanism in these model systems. This aim was pursued by considering the theoretical results of the dynamic disorder hopping models previously proposed[11,12,20−23] in terms of ion hopping and host medium reorganization and by studying the equivalent conductivity in relation to temperature and composition.

The complete interpretation of the data was achieved by a combined approach based on a universal power law (UPL)[7,24] in the framework of the jump−relaxation model[25] and by equivalent circuit analysis.[26] Correlation of these results with the structural determination previously reported[19] allowed us to propose a conductivity mechanism for the PEG400/(LiCl)$_x$ systems.

2. Experimental Section

2.1. Reagents. Metallic lithium powder (~325 mesh, 99.9%), 1-chlorobutane, PEG400, and solvents were supplied by Aldrich and further purified by standard methods, with the exception of lithium (see below). The dehydration of PEG400 was performed under high vacuum at 90 °C for 72 h at 10^{-3} mbar followed by 48 h at 10^{-6} mbar; dehydration was confirmed by the Karl Fisher titration method. All reagents were stored under argon on 4A molecular sieves and transferred and handled in an argon atmosphere.

2.2. Synthesis of LiCl and PEG400/(LiCl)$_x$ Complexes. The preparation of the LiCl salt and PEG400/(LiCl)$_x$ complexes was performed as described more extensively in refs 19 and 27. LiCl was obtained by refluxing 400 mL of 1-chlorobutane that had been mixed with 2.29 g of lithium powder. The resulting thick violet solid was washed with *n*-heptane and dried for 1 day at 140 °C under a vacuum of 10^{-3} mbar. The LiCl salt had the following composition: 16.28% Li, 83.20% Cl, 0.52% metallorganic species. Li was determined by inductively coupled plasma atomic emission spectroscopy (ICP-AES) and Cl by Mohr titration. Both determinations were carried out using a solution of the sample dissolved in bidistilled water.

LiCl (7.71 g) was added to 75 mL of PEG400 in a 100-mL flask and stirred at 80 °C for 2 h. Upon being cooled to room temperature, the liquid obtained was reddish, transparent, homogeneous, and highly viscous. Dilution of this mother solution with PEG400 gave nine PEG400/(LiCl)$_x$ complexes with $0.00207 \leq x \leq 1.40665$. Samples of the polymer electrolytes were dissolved in bidistilled water and their salt contents were measured by ICP-AES using the method of standard additions. Compositional data are given in Table 1.

2.3. Instrumentation. ICP-AES determinations were performed using a Spectroflame Modula sequential and simultaneous spectrometer equipped with a capillary cross-flow nebulizer (Spectro Analytical, Kleve, Germany). The Li content in the samples was measured using a plasma power of 1.2 kW, a radio frequency of 27.12 MHz, and an argon gas flow with nebulizer, auxiliary, and coolant controls set at 1, 0.5, and 14 L/min, respectively. The lithium emission line was measured at 670.784 nm, and the argon reference line was set at 430.01 nm.

TABLE 1: Composition Data for PEG400/(LiCl)$_x$ Complexes[a]

compound	c_{Li} (mol/kg)	$\sqrt{c_{Li}}$ (mol/kg)$^{1/2}$	$x = n_{Li}/n_{PEG}$	$r = n_{Li}/n_O$
1	3.4328	1.85278	1.40665	0.14547
2	1.7202	1.31156	0.69639	0.07202
3	0.8674	0.931343	0.34906	0.03610
4	0.3861	0.621369	0.154855	0.01601
5	0.1922	0.438406	0.07698	0.00796
6	0.09134	0.302225	0.03656	0.00378
7	0.04653	0.215708	0.018618	0.00193
8	0.02276	0.150864	0.009105	0.00094
9	5.186×10^{-3}	0.0720139	0.002074	0.00021

[a] n_{Li}, n_{PEG}, and n_O are the numbers of moles of Li, PEG, and oxygen, respectively, in the complexes.

FT-IR spectroscopy in the mid-infrared region, performed using a Nicolet 5SxC spectrometer equipped with a triglycine sulfate (TGS) detector, permitted us to verify the complete absence of water in the synthesized materials. The samples were prepared under an argon atmosphere in cells equipped with KBr windows.

AC impedance measurements were performed in the interval of frequencies between 20 Hz and 1 MHz by a computer-interfaced HP4284A precision LCR meter equipped with an Amel 192 conductivity cell with two parallel platinum electrodes. Measurements were taken in a temperature range of 20−85 °C; the cell constant was 0.985 cm. The measuring cell with each sample was sealed in a drybox and kept in a strictly argon atmosphere during the measuring period. Conductivity data were determined from complex impedance measurements using the "equivalent circuit" software package developed by Boukamp[28] and the equivalent circuit model reported in ref 27. The calculated resistance values were affected by an error of less than 3%.

3. Results and Discussion

3.1. Observations on PE Preparations. The conducting properties of polymer electrolytes are strongly affected by the solvent used in the preparation of the materials.[8] To avoid these interferences, the electrolytic systems examined here were prepared by dissolving a LiCl salt directly in PEG400, which can be treated as unique solvent having cooperative solvation ability. This LiCl salt was prepared as described in ref 19 by the following simple single-step reaction:

$$Li_{(s)} + \text{1-chlorobutane}_{(l)} \xrightarrow[\text{(b) } \Delta\text{, reflux}]{\text{(a) argon atmosphere}} LiCl_{(s)}$$

This reaction yields LiCl that is highly anhydrous and more reactive toward Lewis bases compared to the rigorously purified, commercially available product. Indeed, XRD measurements demonstrated that this salt is characterized by a high degree of crystallographic disorder.[19] These properties allowed us to prepare nine very pure PEG400/(LiCl)$_x$ polymer electrolytes ($0.00207 \leq x \leq 1.40665$), without any need for solvents other than PEG400. Details on the composition of each PE material are reported in Table 1.

3.2. Impedance Measurements and Conductivity Spectra. Practical application of PE technology to the construction of

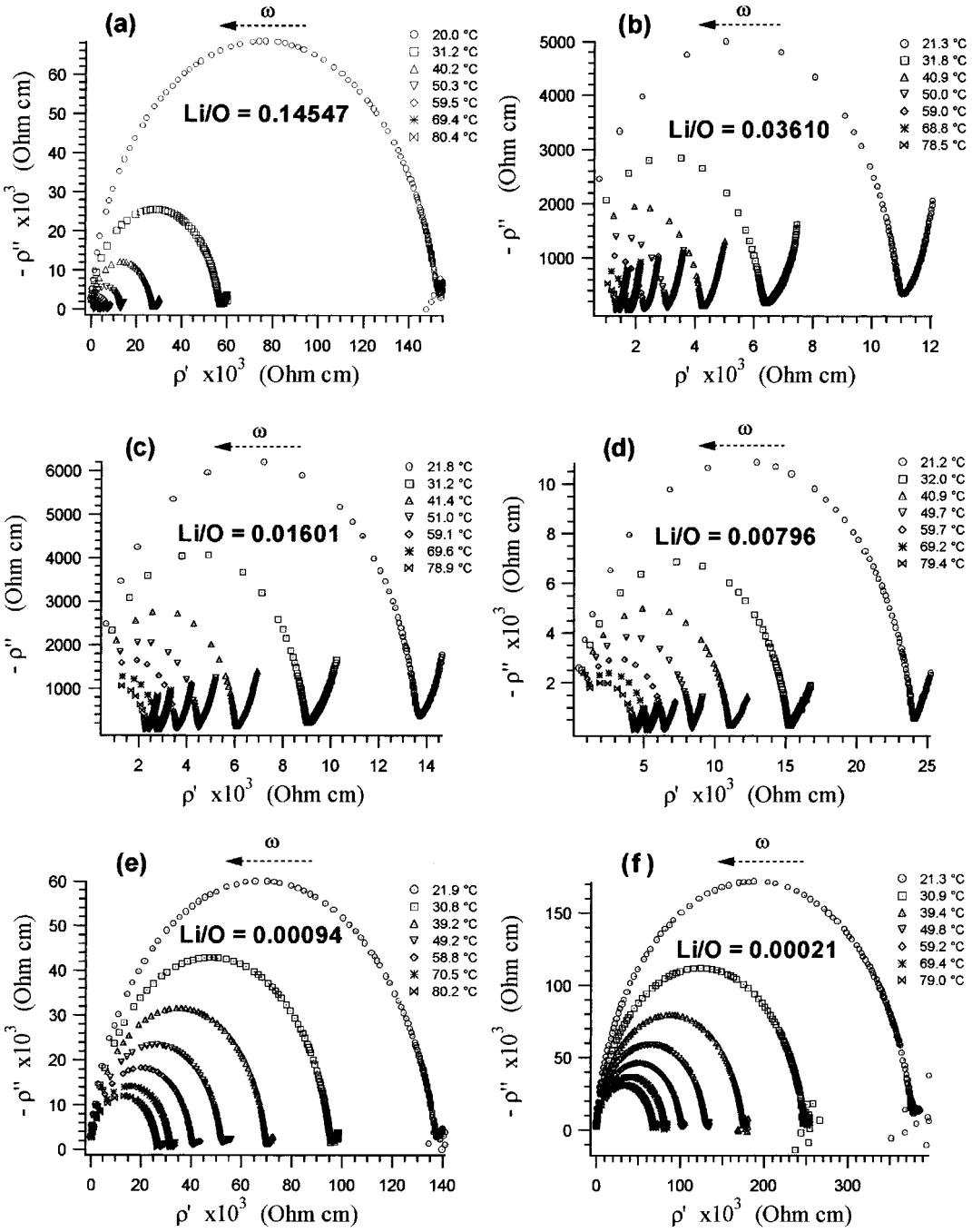

Figure 1. Nyquist plots of selected (PEG400)/$(LiCl)_x$ complexes at various temperatures. The measurements were carried out from 20 Hz to 1 MHz.

lithium batteries requires a full characterization of the material's AC response.[1−3] Therefore, to meet these requirements and to characterize the conductivity mechanism in the nine (PEG400)/$(LiCl)_x$ complexes, we first turned our attention to a complete analysis of their impedance spectra. Figure 1 presents Nyquist plots derived at various temperatures for some PE materials of Table 1. A careful inspection of the curves reveals the presence of semicircular arcs at high frequencies, which are attributed to the bulk properties of the material; spikes attributed to diffusion-limited Warburg impedances[29] are present at low frequencies. The temperature and composition strongly influence the frequency range of the profiles. The presence of a single semicircle is typical of a geometrical capacitance and a bulk resistance in parallel with it. Data simulations were next carried out using the EQUIVCRT program[28] by adopting different equivalent circuit (EC) models; constant phase elements (CPEs) for both the capacitance and Warburg element were initially used in the calculation procedure. Results indicated that the impedance spectra are well reproduced if an equivalent circuit consisting of a parallel impedance in series with a Warburg diffusion-limited impedance is used. In this EC, the parallel impedance is constituted by a resistance in parallel with a capacitance. The resulting n values calculated for all of the polymers at all temperatures were close to unity for the CPEs in parallel and close to 0.5 for CPEs in series with the parallel circuits, thus confirming the above assignment. Furthermore, the capacitance of ca. 1.5×10^{-10} F measured for the parallel circuit was independent of the composition and temperature of the sample. These findings indicate that the main spectral changes observed in Figure 1 are directly related to the resistance variations in

the samples. By using the bulk resistance thus determined, we were able to calculate the conductivities of the PE samples as a function of temperature.

By making use of the impedance data and the equation[7]

$$\sigma'(\omega) = Z'(\omega)/k[(Z'(\omega))^2 + (Z''(\omega))^2]$$

where k is the cell constant in centimeters, we evaluated the real component of the conductivity, $\sigma'(\omega)$. The $\sigma'(\omega)$ spectra of three PE samples are shown in Figure 2. These profiles are characterized by three different regions: (a) the low-frequency spike, (b) the medium-frequency plateau, and (c) the high-frequency spike. The R, C, and Warburg element parameters determined by the EC analysis described above simulate very well the medium plateau and low-frequency spike of the $\sigma'(\omega)$ plots. However, the high-frequency portion of the $\sigma'(\omega)$ curves, which depends on the temperature and sample composition, cannot be described by the simple equivalent circuit analysis described above. The steep increase in $\sigma'(\omega)$ at high frequencies was attributed to correlated ionic motions in the PE bulk materials, as suggested in other studies.[22−25,30,31] Indeed, analogous $\sigma'(\omega)$ profiles at high frequencies were previously observed for structurally disordered inorganic solid materials.[22,23,25,30,31] To fully characterize the AC electrical response of the (PEG400)/(LiCl)$_x$ complexes, it was necessary to analyze the data in terms of both EC analysis and correlated ionic motions based on the jump relaxation model. This latter analysis was carried out by fitting the $\sigma'(\omega)$ data at frequencies higher than 1 kHz with a universal power law (UPL) equation[24,31]

$$\sigma'(\omega) = \sigma'(0)[1 + (\omega\tau_1)^p] \qquad (1)$$

where $\sigma'(0)$ denotes the DC conductivity ($\sigma'(0) \cong \sigma_{DC}$), τ_1 is a time related to the initial site relaxation time of ion hopping τ_2, $p = \tau_2/\tau^*$ is the power law exponent, and τ^* is the initial back-hop relaxation time. Curves obtained by fitting the data using nonlinear least-squares methods (represented by dotted lines in Figure 2) clearly show that eq 1 fits the $\sigma'(\omega)$ data very well at frequencies higher than ca. 1 kHz.

Further confirmation of the applicability of the UPL equation was attained by plotting both $\sigma'(\omega)/\sigma'(0)$ and $\ln[\sigma'(\omega)/\sigma'(0) - 1]$ against logarithms of frequency.[7] Figure 3a shows that, for all temperatures and sample compositions, $\sigma'(\omega)/\sigma'(0)$ presents a central plateau close to unity. At high frequencies, $\sigma'(\omega)/\sigma'(0)$ increases steeply depending on the temperature and PE composition. This representation leads us to expect a linear dependence of $\ln[\sigma'(\omega)/\sigma'(0) - 1]$ on $\log(f/\text{Hz})$ at high frequencies, a prediction that was confirmed experimentally (Figure 3b). The UPL dependence of $\sigma'(\omega)$ at high frequencies was explained by a physical model for structurally disordered ionic conductors.[22,23,31] In this model, called the jump relaxation model, each mobile ion in the bulk material experiences an effective potential that is the result of the superposition of a periodic lattice potential and a "cage effect" potential caused by Coulomb interactions with charge carriers. This model predicts the existence of at least two different kinds of sites, indicated by A and C,[31,32] which are more or less likely, respectively, to host the mobile ion. In this framework, if the ion performs a hop from site A to site C, the effective potential minimum remains in A. Therefore, two competing relaxation phenomena can occur. First, the ion can hop back to A, giving no contribution to the conductivity ("unsuccessful hop"). During this back-hop relaxation, the effective potential remains unchanged,[30] and the kinetics are regulated by the time constant τ^*. Alternatively, the dipoles that give rise to the coordinating

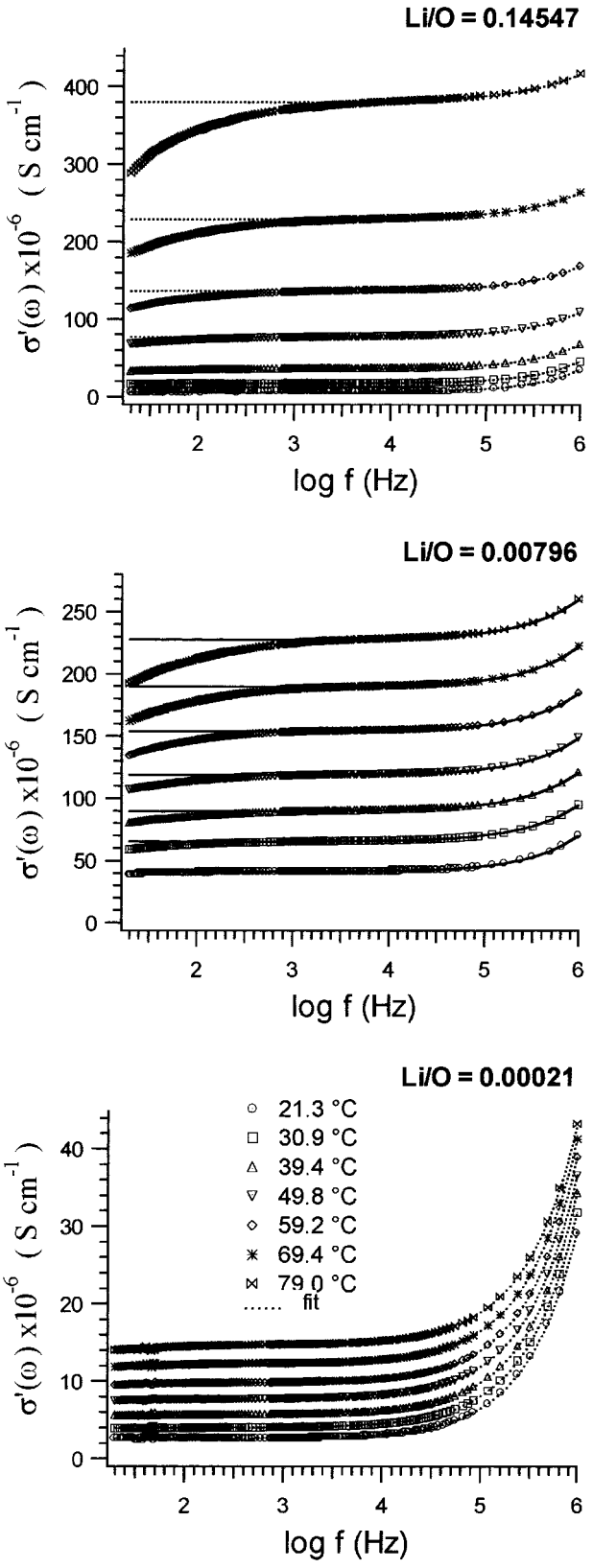

Figure 2. Real conductivity component, $\sigma'(\omega)$, versus log f (Hz) of selected (PEG400)/(LiCl)$_x$ measured at various temperatures. Dotted lines show the curves obtained by fitting $\sigma'(\omega) = \sigma'(0)[1 + (\tau_1\omega)^p]$ to $\sigma'(\omega)$ using experimental data obtained at frequencies higher than 1 kHz. The data were fitted using nonlinear least-squares procedures.

"cage" structure can relax through correlated events, shifting the cage effect minimum toward the new site C, thus creating a new absolute potential minimum. This second type of initial

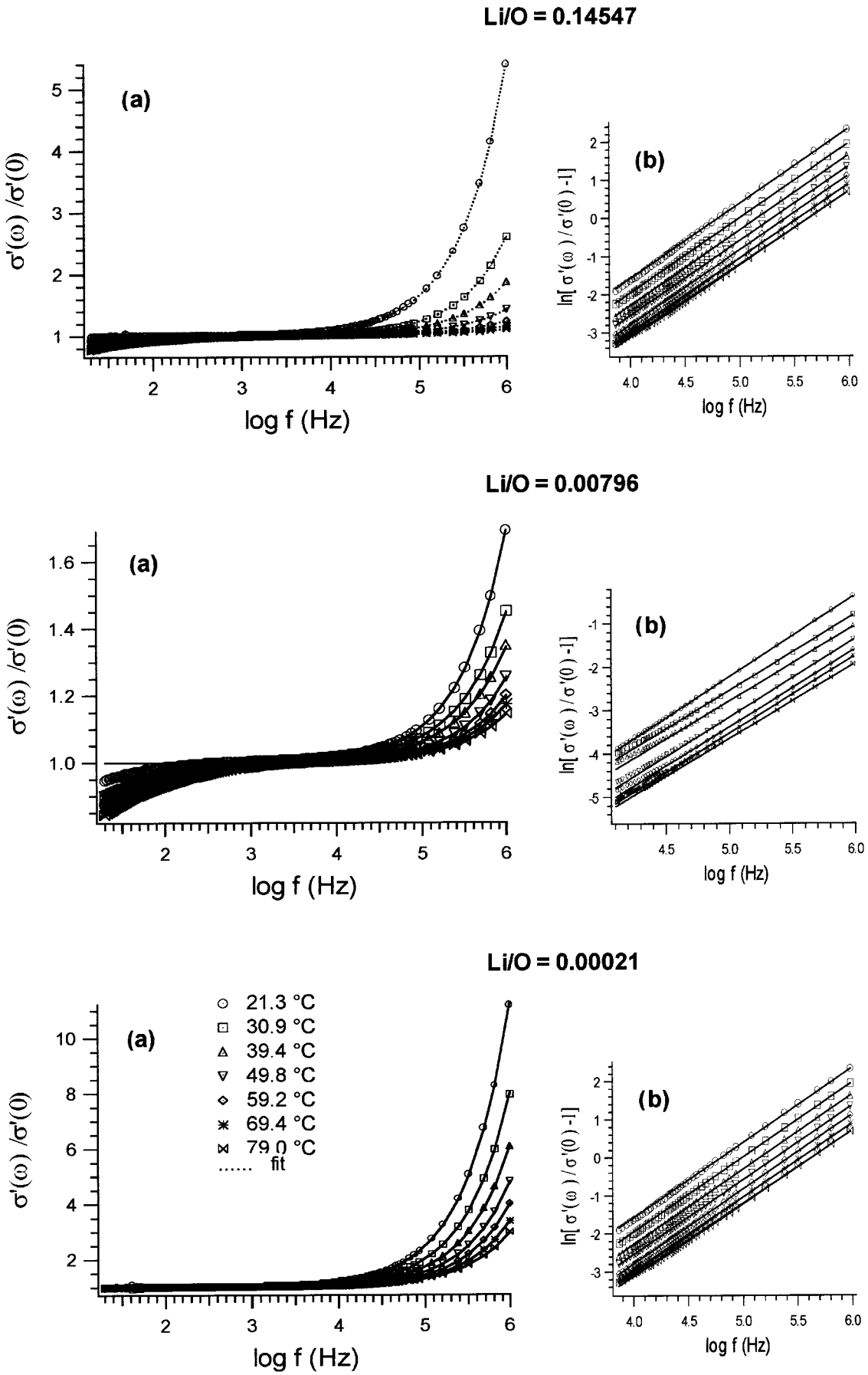

Figure 3. (a) $\sigma'(\omega)/\sigma'(0)$ as a function of log f (Hz); (b) $\ln[\sigma'(\omega)/\sigma'(0) - 1]$ versus log f (Hz). The simulated curves are shown by dotted lines.

ion hopping is referred to as "successful" because it contributes to the total conductivity. The kinetics of this process are described by τ_2 (the site relaxation time). On the basis of this definition, the power-law exponent of eq 1 was interpreted as

τ_2/τ^*.[31] The same authors suggested that site relaxation takes place through two distinct processes, namely, a shift of the Coulomb cage (as usually happens) and a geometrical relaxation caused by host network adjustment.[22,23,31] Therefore, the determination of parameter p in eq 1 is a crucial point for studying the relaxation mechanism and the relative influence of backhop and site relaxation processes on the overall conductivity mechanism.[7] The polymer electrolytes investigated here present two characteristics: first, they are below the entanglement limit, thus indicating that the oligomer macromolecules are highly mobile in the material, and second, the oxygen coordination sites are located linearly along the PEG400 chain axis.[19] Thus, these materials could be considered as composites of highly mobile empty PEG400 chains, complex cations of the type $[PEG400/Li]^+$, and Cl^- ions both involved in hydrogen-bonding cages with terminal OH groups of PEG chains and distributed as free anions between the polyetheric chains. For simplicity, we refer to all of the sites present in the same chain of the complex $[PEG400/Li]^+$ as A sites and to all of the coordination positions located along the axis of the empty PEG400 macromolecules surrounding the complex $[PEG400/Li]^+$ as C sites. The hops between A sites do not require any substantial host medium reorganization. Interchain hopping events between A and C sites are expected to take place on two distinct time scales, the first associated with the instantaneous hops, and the second with the time involved in host medium reorganization.[12,20,21] On the other hand, as described above and in agreement with other proposed dynamic disorder models for conductivity,[12,20,21] host medium reorganization processes could be attributed to two phenomena. The first phenomenon describes the ionic correlation events between the complex cations $[PEG400/Li]^+$ and the Cl^- anions distributed in the bulk material, and the second is associated with the reorganizations occurring after hopping of all those dipoles that are involved in the coordination cage structures of cations and anions. All of these host medium reorganization events are expected to take place with ease if the polymer electrolyte is prepared using macromolecules below the entanglement regime.

Furthermore, the plots of $-\rho''(\omega)$ versus the logarithms of frequency reveal the presence of typical Debye peaks.[26] Figure 4 shows that the frequency of the maximum of these Lorentzian shapes depends on the PE composition and temperature. Fitting these profiles by Lorentzian functions allowed us to measure τ_{peak} at the maximum height of the peaks and to establish the relationships between the conductivity relaxation times[26] $\tau_{peak} = 1/f_{peak}$ and both the temperature and the composition of the (PEG400)/(LiCl)$_x$ systems.

To acquire information about the conductivity mechanism, the parameters determined using the EC and UPL analyses were analyzed in depth as a function of temperature and Li concentration in the PE materials.

The dependence of the conductivities $\sigma_{VTF}(T)$ and $\sigma'(0)$ on the reciprocal absolute temperature are reported in Figure 5. As expected, the values for $\sigma_{VTF}(T)$ determined from the EC analysis coincide exactly with $\sigma'(0)$ obtained by fitting the high-frequency $\sigma'(\omega)$ data with eq 1. Furthermore, both $\sigma_{VTF}(T)$ and $\sigma'(0)$ present the typical temperature-dependent relation described by the empirical Vogel−Tamman−Fulcher (VTF) equation[9]

$$\sigma_{VTF}(T) = A_\sigma T^{-1/2} e^{-E_{VTF}/R(T-T_0)} \qquad (2)$$

where A_σ is proportional to the number of carrier ions, R is the gas constant, E_{VTF} is a constant proportional to the activation energy for conduction, and T_0 is the thermodynamic ideal glass transition temperature at which the configurational entropy becomes zero or the "free volume" disappears.[9] It is to be pointed out that the exact coincidence of σ_{VTF} and $\sigma'(0)$ clearly indicates that the medium-frequency plateau of the $\sigma'(\omega)$ spectra is well described by both the EC and UPL models. The dependence of the conductivity on the reciprocal of the absolute temperature in this region is well described by eq 2, as illustrated by the dotted curves shown in Figure 5. These curves were

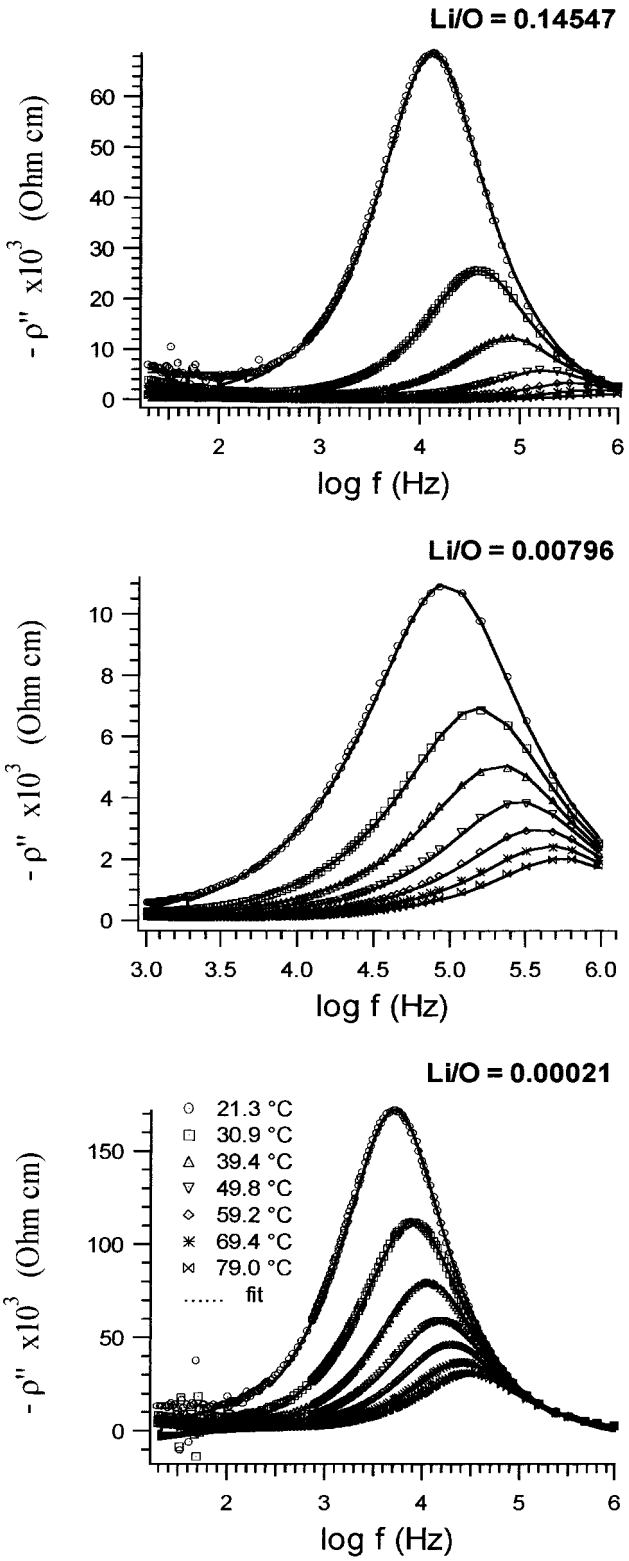

Figure 4. Imaginary component of the complex resistivity, $-\rho''(\omega)$, versus log f (Hz) for selected (PEG400)/(LiCl)$_x$ complexes.

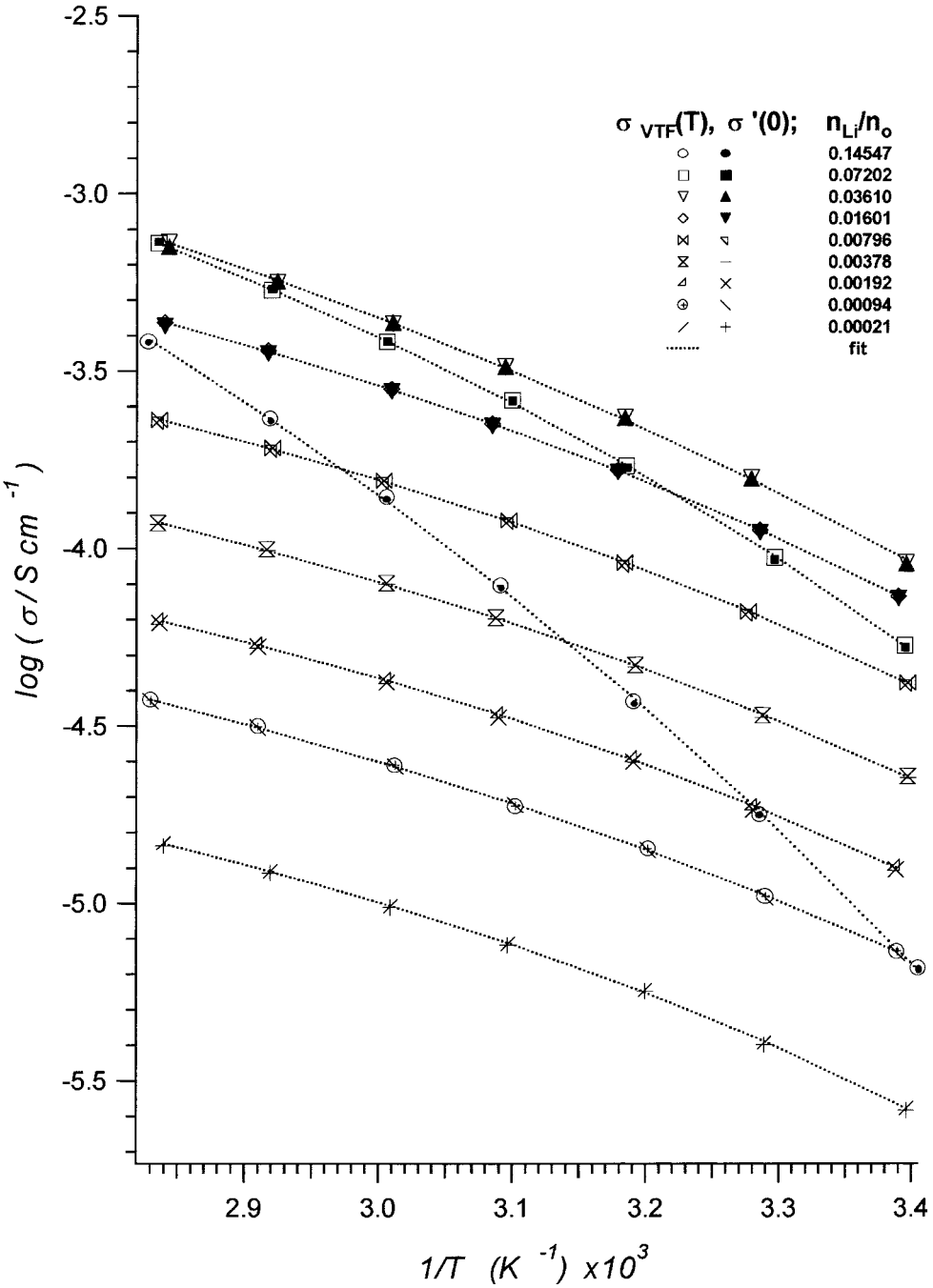

Figure 5. Dependences of log σ_{VTF}(T) and log σ'(0) on temperature. Dotted lines show VTF fitted curves.

determined by fitting eq 2 to the conductivity data by means of nonlinear least-squares methods and assuming a starting T_0 value on the basis of the boundary condition $(T_g - 55) \leq T_0 \leq (T_g - 40)$, $T_g \approx -60$ °C, as suggested in the literature.[19,9]

Figure 6a and b reports the dependence of A_σ, T_0 and E_{VTF} on concentration, $c_{Li}^{1/2}$ (mol/kg)$^{1/2}$. It is to be observed that A_σ and E_{VTF} increase monotonically and T_0 decreases as the salt concentration increases. Two conductivity regions can be distinguished: region I, detected for $0.0021 \leq r \leq 0.0160$ or $0.072 \leq c_{Li}^{1/2} \leq 0.6214$, and region II for $r \geq 0.0361$ or $c_{Li}^{1/2} \geq 0.9313$ (mol/kg)$^{1/2}$. In region I, A_σ, T_0, and E_{VTF} are practically independent of composition, whereas in region II, E_{VTF} and A_σ, exhibit an exponential steep increase and T_0 decreases as $c_{Li}^{1/2}$ (mol/kg)$^{1/2}$ increases. These results could be rationalized if we take into account the ion−PEG400 interactions and the structural results previously reported for FT-IR investigations of (PEG400)/$(LiCl)_x$ systems.[19] Indeed, it has been demonstrated that the PEG400 chains exhibit a TGT (T = trans, G = gauche) conformation and that Li^+ ions are accommodated in the coordination sites provided by the ethereal oxygen atoms present along the TGT chains of PEG400.[19] These two properties are not influenced by the concentration of LiCl in the PE. However, the salt substantially modifies the hydrogen-bonded bulk structure of the pristine PEG400. In contrast, the (PEG400)/$(LiCl)_x$ bulk structure is influenced by the Cl^- anion, which (a) for $0.072 \leq c_{Li}^{1/2} \leq 0.6214$ (mol/kg)$^{1/2}$, gives rise to hydrogen-bonding clusters with the terminal hydroxyls of PEG chains;[19] and (b) for $c_{Li}^{1/2} \geq 0.9313$ (mol/kg)$^{1/2}$, remains preferentially involved in hydrogen-bonding clusters with the terminal OH groups of PEG400, but with a fraction of the total Cl^- ion concentration distributed along the PEG400 chains, thus giving rise to the so-called free anion concentration.[19] A portion of

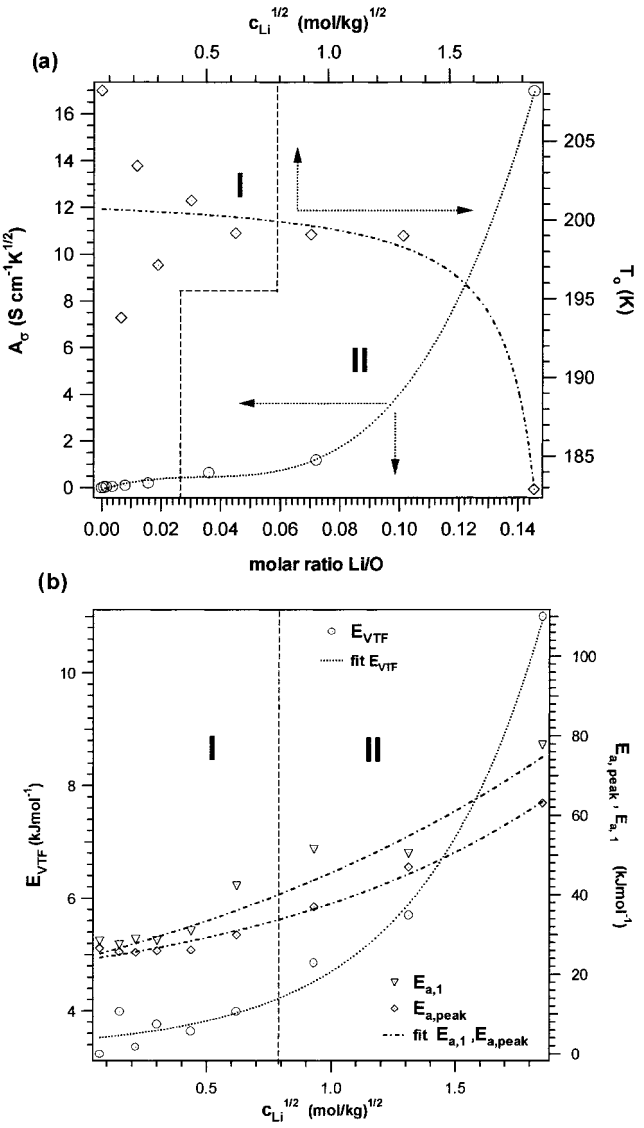

Figure 6. (a) A_σ and T_0 as functions of salt concentration for (PEG400)/(LiCl)$_x$ complexes; (b) E_{VTF}, $E_{a,peak}$, and $E_{a,1}$ as functions of salt concentration.

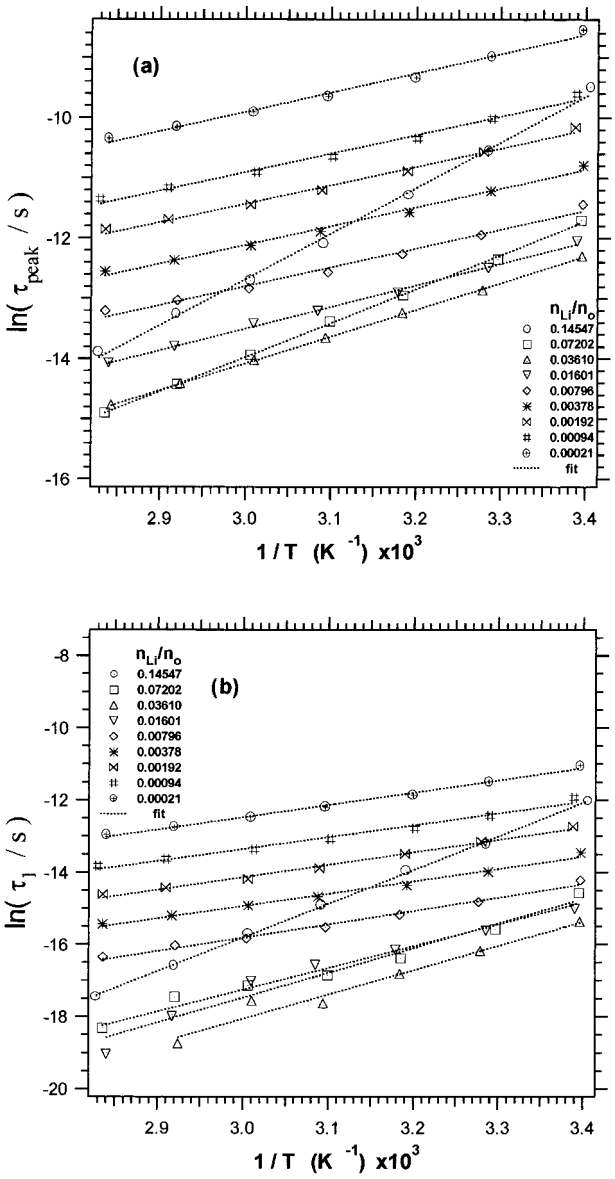

Figure 7. Dependences of ln τ_{peak} and ln τ_1 on $1/T$ for (PEG400)/(LiCl)$_x$ complexes.

this free anion concentration is involved in the formation of Li−Cl ionic couples. This model clearly explains the results shown in Figure 6 by suggesting that, when $c_{Li}^{1/2}$ is higher than 0.9313 (mol/kg)$^{1/2}$, the formation of extended dynamic PEG−LiCl−PEG cross-links in PE materials reduces T_0, raises the fitting parameter E_{VTF}, and markedly increases A_σ (A_σ depends on the concentration of free ionic carriers). On the other hand, at $c_{Li}^{1/2}$ lower than 0.6214 (mol/kg)$^{1/2}$ (region I), A_σ, T_0, and E_{VTF} are practically independent of concentration. These observations suggest that, in this PE composition range, the conductivity could be associated with the presence of a constant concentration of "free ionic carriers". We feel that this constant concentration of carriers is generated by an equilibrium of the type

$$\text{bonded ions} \leftrightarrow \text{free ionic carriers} \qquad (3)$$

which takes place in the bulk PE material. According to the vibrational results reported in the literature,[19] we believe that this equilibrium modulates the concentration of free ionic carriers, which are responsible for the conductivity, and is generated by the Cl^- ions involved in the formation of hydrogen-bonded clusters (bonded ions) and those freely distributed along the PEG400 chains (the free ionic carriers). Indeed, migration of a lithium ion toward the cathode requires the simultaneous movement of a corresponding anionic charge in the opposite direction. This means that chloride ions must be distributed freely along the PEG400 chains as free anions.

Additional information on the conductivity mechanism in these systems is obtained studying the relaxation times τ_{peak} and τ_1 determined from the Debye peaks (Figure 4) and from the fitting of eq 1 to the $\sigma'(\omega)$ data (Figure 2), respectively. An accurate analysis of Figure 7a and b shows that the temperature dependences of τ_{peak} (the conductivity relaxation time) and τ_1 (a time correlated to the initial site relaxation time τ_2, see eq 1) are of the Arrhenius type

$$\tau_{peak} = \tau_{0,peak} e^{E_{a,peak}/RT} \qquad (4)$$

$$\tau_1 = \tau_{0,1} e^{E_{a,1}/RT} \qquad (5)$$

where $\tau_{0,peak}$ and $\tau_{0,1}$ are preexponential constants, $E_{a,peak}$ is the activation energy for the thermally stimulated conductivity

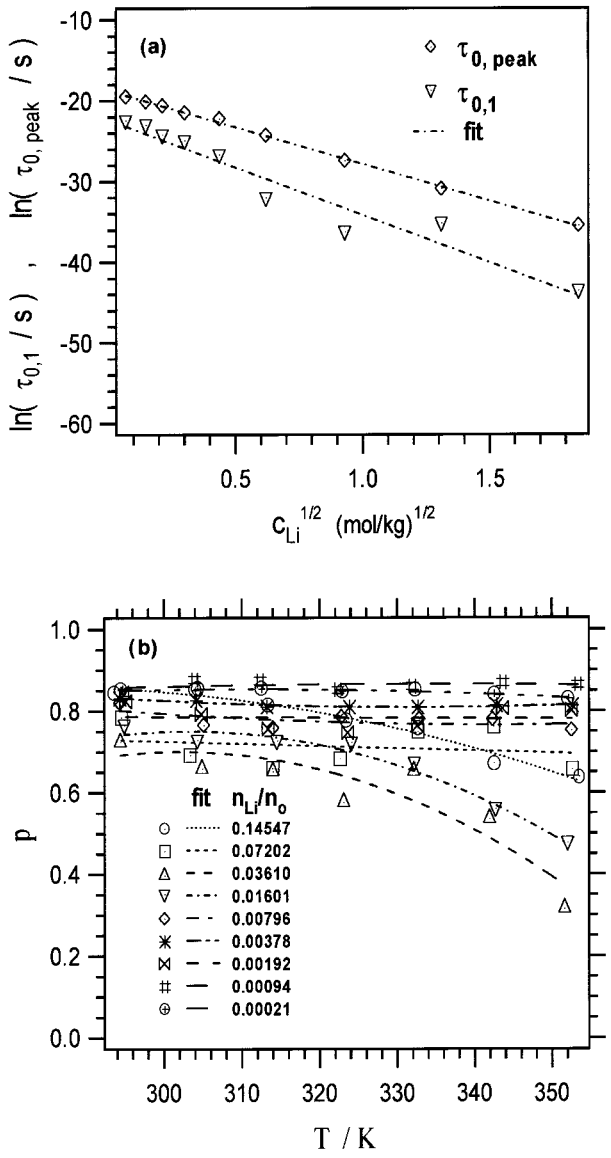

Figure 8. (a) ln $\tau_{0,1}$ and ln $\tau_{0,peak}$ versus the concentration of (PEG400)/$(LiCl)_x$ complexes; (b) plot of p as a function of the reciprocal of temperature.

relaxation time, and $E_{a,1}$ is the site relaxation energy height barrier. Figure 7a and b also shows that these parameters allow us to identify the same two regions of conductivity discussed above. The Arrhenius parameters of eq 4 and 5 determined by fitting the data of Figure 7a and b are plotted as a function of temperature in Figures 6b and 8a. Figure 8a reveals that the natural logarithms of the preexponential factors $\tau_{0,1}$ and $\tau_{0,peak}$ are linearly dependent on $c_{Li}^{1/2}$ (mol/kg)$^{1/2}$

$$\ln \tau_{0,i} = \lambda_i - \beta_i c_{Li}^{1/2} \quad i = 1, \text{peak} \tag{6}$$

where the fitting parameters are $\lambda_1 = -22.3 \pm 2$ and $\beta_1 = -11.79 \pm 1$ (mol/kg)$^{-1/2}$ for $\tau_{0,1}$ and $\lambda_{peak} = -18.7 \pm 0.1$ and $\beta_{peak} = -9.12 \pm 0.08$ (mol/kg)$^{-1/2}$ for $\tau_{0,peak}$. It is to be observed that $\lambda_1 \cong \lambda_{peak}$ at infinite dilution, thus indicating that, under these conditions, the conductivity relaxation time coincides with the initial site relaxation time. On the other hand, as $c_{Li}^{1/2}$ increases, ln $\tau_{0,i}$ ($i = 1$ and peak) decreases monotonically, because of the ion−ion and ion−PEG400 interactions (Figure 8a).

TABLE 2: Parameters Determined by Fitting Equations 7[a] to the Data Reported in Figure 6b

i	E_i^0 (kJ mol^{-1})	α_i (kJ mol^{-1})	γ_i (mol/kg)$^{-1/2}$
VTF	3.32 ± 0.06	0.19 ± 0.08	2.0 ± 0.1
a,peak	12.2 ± 1	11.4 ± 0.7	0.81 ± 0.05
a,1	21.0 ± 1	5.8 ± 0.5	1.2 ± 0.1

[a] $E_i^0 = E_i^0 + \alpha_i e^{\gamma_i c^{1/2}}$, where i = VTF; a,peak; a,1.

Furthermore, the pseudo activation energies calculated from the conductivity data (E_{VTF}) and the activation energies determined from the conductivity relaxation times ($E_{a,peak}$) and initial site relaxation times ($E_{a,1}$) exhibit the same functional dependence on $c_{Li}^{1/2}$. Specifically, they are well represented by

$$E_{VTF} = E^\circ_{VTF} + \alpha_{VTF} e^{\gamma_{VTF} c_{Li}^{1/2}}$$

$$E_{a,peak} = E^\circ_{a,peak} + \alpha_{a,peak} e^{\gamma_{a,peak} c_{Li}^{1/2}}$$

$$E_{a,1} = E^\circ_{a,1} + \alpha_{a,1} e^{\gamma_{a,1} c_{Li}^{1/2}} \tag{7}$$

Table 2 reports the parameters determined by fitting eq 7 to the data plotted in Figure 6b. It is to be noticed that in region I, $E_{a,peak}$ is approximately equivalent to $E_{a,1}$ ($E_{a,peak} = E^\circ_{a,peak} + \alpha_{a,peak}$; $E_{a,1} = E^\circ_{a,1} + \alpha_{a,1}$), thus confirming the $\tau_{0,i}$ results at low $c_{Li}^{1/2}$ values and suggesting that, in this region, the site relaxation processes coincide with the conductivity relaxation process. If we take into account that the value of the constant E_{VTF} in the second region is always lower than those of the site and conductivity relaxation events, we must recognize that the motions of the PEG400 chains in the bulk material represent a determining factor in the conduction mechanism. All of these observations again demonstrate that the conductivity is mainly regulated by the movement of the polymer chain and by the free charge carriers described above.

Further support for this mechanism is provided by analyzing the temperature dependence of the parameter $p =$ (initial back-hop rate/initial site relaxation rate).[31] Conductivity due to ion hopping is successful when the initial site relaxation rate, $1/\tau_1 = r_s$, in the host material is higher than the initial back-hop rate, $1/\tau^* = r_b$, of the ion.[31,7] Figure 8b shows that this requirement is always satisfied and that (a) at temperatures lower than 315 K, p is similar for regions I and II and close to ~0.8, and (b) at temperatures higher than 315 K, the p profile of samples in region I is unchanged and those of the samples in region II present a continuous decrease. These results reveal that ion hopping with consequent site relaxation contributes significantly to the overall conductivity of PE materials and that, for the samples of conductivity region II, the process of site relaxation after hopping is favored at high temperatures with respect to back-hopping relaxation. Taken together, these findings strongly suggest that conductivity occurs as a result of hopping events followed by site relaxation processes, whose contribution to the overall conductivity of PE is mainly regulated by the segmental motion of the host material.

3.3. Equivalent Conductivity Studies. To detect the possible ion association interactions in (PEG400)/$(LiCl)_x$ systems, we performed an in-depth analysis of the equivalent conductivity with respect to the LiCl concentration, $c_{Li}^{1/2}$ (mol/kg)$^{1/2}$. The isothermal equivalent conductivity $c_{Li}^{1/2}$ curves are depicted in Figure 9a. It is to be highlighted that also in this case two distinct conductivity regions are detected as a function of concentration. Region I, which is observed at $c_{Li}^{1/2} \leq 0.6214$ (mol/kg)$^{1/2}$, exhibits an exponential decrease in the equivalent conductivity.

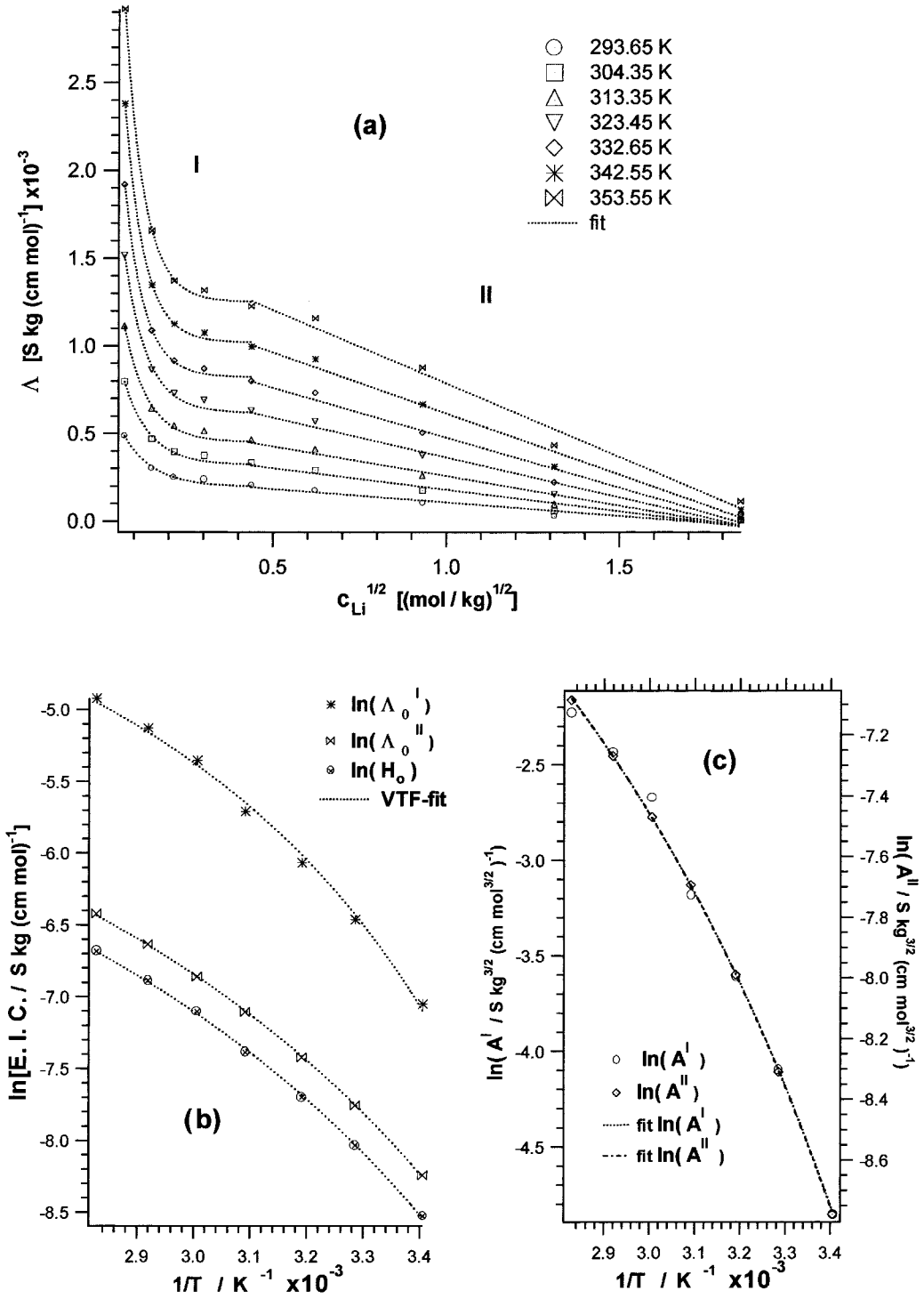

Figure 9. (a) Equivalent ionic conductivity as a function of salt concentration in (PEG400)/(LiCl)$_x$ complexes. (b) Equivalent ionic conductivity at infinite dilution (E. I. C.) versus the reciprocal of temperature. (c) Slopes (A^I and A^{II}) of the Onsager-type equations as functions of $1/T$.

These curve shapes are well-described by an equation of the type

$$\Lambda^I = H_0 + Ke^{-\alpha c_{Li}^{1/2}} \tag{8}$$

where H_0, K, and α are fitting parameters and Λ^I is the equivalent conductivity in region I. These Λ^I profiles show the typical decrease already observed for other polymer electrolyte systems.[1,33] In the literature,[1] this sharp decrease in Λ has been attributed to strong cation−anion interactions, resulting in the formation of electrically neutral ion pairs.[1,33,34] For $c_{Li}^{1/2} \ll 1$ (mol/kg)$^{1/2}$, eq 8 approximates an Onsager-type relation[34]

$$\Lambda^I = \Lambda_0^I - A^I c_{Li}^{1/2} \tag{9}$$

where $\Lambda_0^I = H_0 + K$ and $A^I = K\alpha$.

The dependences of Λ_0^I and H_0 on the inverse absolute temperature are reported in Figure 9b. An interesting result is that Λ_0^I and H_0, which correspond to the equivalent conductivity at infinite dilution, exhibit typical VTF behavior, thus indicating that they are correlated with the Stokes mobility, i.e., with the chain mobility.[34] In region II, the equivalent conductivity

TABLE 3: Parameters Determined by Fitting Λ^{I} and Λ^{II} Data of Figure 9b with the VTF Type Equation $\Lambda_0^i(T) = \Lambda_{0,0}^i T^{-1/2} \exp[-E_{a,\Lambda^i}/R(T - T_0^i)]$ (i = I, II)

i	$\Lambda_{0,0}^i$ [S kg(cm mol)$^{-1}$]	E_{a,Λ^i} (kJ mol^{-1})	T_0^i (K)
I	0.514 ± 0.002	3.450 ± 0.001	213.1 ± 0.4
II	0.07 ± 0.03	2.924 ± 0.001	213.2 ± 0.1

decreases linearly with $c_{Li}^{1/2}$, following an Onsager-type equation of the form

$$\Lambda^{II} = \Lambda_0^{II} - A^{II} c^{1/2} \qquad (10)$$

where Λ_0^{II} is the conductivity at infinite dilution and A^{II} is a constant related to Λ_0^{II}. Such, Λ^{II} profiles are unexpected. Indeed, in other PE systems,[1,33] the concentration dependence of Λ^{II} initially presents an increase in equivalent conductivity that is attributed to the formation of charged triple ions. This stage is followed by a decrease attributed to the formation of transient interchain cross-links. These latter interactions increase the viscosity of the material, giving rise to a more rigid PE matrix.[1,33,34]

An Onsager-type behavior described by eq 10 is observed for (PEG400)/$(LiCl)_x$ materials in region II. In accordance with other studies,[1,33,34] this dependence was attributed to a decrease in the dielectric constant of the material, which is correlated with the increase in viscosity.[34] Both of these phenomena indicate that, in region II, increasing the salt concentration in the (PEG400)/$(LiCl)_x$ complexes results in the formation of transient interchain cross-links that reduce the Λ^{II} of the material. Figure 9b shows that the dependences of Λ_0^{I}, Λ_0^{II}, and the slopes (Figure 9c) of the Onsager-type equations on temperature are well reproduced by VTF equations, indicating that, independent of the presence or absence of ion−ion interactions, segmental motion is a determining factor for the (PEG400)/$(LiCl)_x$ conductivity. The parameters determined by fitting the data of Figure 9b with the typical temperature-dependent behavior described by empirical Vogel−Tamman−Fulcher (VTF) equations are reported in Table 3. These parameters are represented by

$$\Lambda_0^i(T) = \Lambda_{0,0}^i T^{-1/2} \exp[-E_{a,\Lambda^i}/R(T - T_0^i)] \qquad (11)$$

where $\Lambda_{0,0}^i$ is a preexponential constant, E_{a,Λ^i} is the pseudo activation energy for conduction at infinite dilution, and T_0^i is the ideal glass transition temperature; regions I and II are denoted by the superscript index i. Table 3 shows that the values for T_0 in regions I and II are very close to the nominal T_g value of pure PEG400 and that the pseudo activation energies so determined are similar to those obtained from the conductivity data at infinite dilution (Table 2).

4. Conclusions

This report describes the preparation of very pure solvent-free liquid polymer electrolytes having the composition (PEG400)/$(LiCl)_x$ with $0.02074 \le x \le 1.40665$ and their characterization by complex impedance spectroscopy.

Detailed analysis of the real and imaginary components of the conductivity of the (PEG400)/$(LiCl)_x$ complexes indicated that a full characterization of the AC electrical response of these complexes requires both equivalent circuit analysis and correlated ionic motion analysis carried out using the UPL equation.

Both of these investigations indicated that the conductivity of the prepared PE is ionic and takes place through two distinct phenomena, i.e., the hopping of charge carriers between the sites present in the material along the polyethereal chain (intra-CH hopping) and the migration of the ions between different PEG400 chains (inter-CH hopping). As described in the literature,[7,31] this hopping results in conduction if the coordination site that accommodates the ion after the hopping is in a relaxed state. It was demonstrated that this inter-CH event is strongly preferred and is dependent on the segmental motion of the polymeric chains.

Moreover, it was revealed that the (PEG400)/$(LiCl)_x$ complexes exhibit two conductivity regions; region I was detected for $0.072 \le c_{Li}^{1/2} \le 0.6214$ (mol/kg)$^{1/2}$ and region II for $c_{Li}^{1/2} \ge 0.9313$ (mol/kg)$^{1/2}$. The ionic interactions in these two regions were detected by analyzing the equivalent conductivity of (PEG400)/$(LiCl)_x$ complexes as a function of temperature and composition.

On the basis of the spectroscopic investigations reported in the literature[19,35] and the results elucidated here, we propose the following configuration for our PE complexes: (a) Li^+ ions are always accommodated in the coordination sites formed by the ethereal oxygens of PEG400 chains in the TGT conformation, with migration of these ions occurring primarily through hopping between coordination sites; (b) the inter-CH hopping, which is a determining factor for the conductivity of the PE, is strongly influenced by the segmental motion of the polyethereal chains and is assisted by the presence of free Cl^- ions distributed along the PEG400 chains. This free Cl^- ion concentration in region I is modulated by an equilibrium between Cl^- involved in the formation of hydrogen-bonding clusters with OH terminal groups of PEG chains and those freely distributed along the polyether chains. Together with Li^+, these free Cl^- ions give rise to so-called solvent-separated ion pairs. In region II, the high salt concentrations reduce the free Cl^- concentration by transforming the solvent-separated ion pairs into contact ion pairs, which are responsible for the dynamic PEG−LiCl−PEG cross-links.[1] The presence of these cross-links in region II increases the viscosity of the material and decreases the equivalent conductivity.

Furthermore, a comparison between the pseudo activation energies of the VTF, conductivity relaxation, and site relaxation energies strongly indicates that the mechanism of conduction most likely involves segmental motion of the PEG400 chains. Finally, it is to be highlighted that the (PEG400)/$(LiCl)_x$ polymers present conductivities on the order of 10^{-4} Scm^{-1} at 25 °C, thus allowing us to classify these materials as good liquid polymer electrolytes.

References and Notes

(1) Gray, F. M. *Polymer Electrolytes*; RSC Materials Monographs; Royal Society of Chemistry: Cambridge, U.K., 1997.
(2) Scrosati, B.; Neat, R. J. *Applications of Electroactive Polymers*; Scrosati, B., Ed.; Chapman and Hall: London, 1993; p 182.
(3) Wright, P. W. *Electrochim. Acta* **1998**, *43*, 1137.
(4) Di Noto, V. *J. Mater. Res.* **1997**, *12*, 3393.
(5) Di Noto, V.; Furlani, M.; Lavina, S. *Polym. Adv. Technol.* **1996**, *7*, 759.
(6) Münchow, V.; Di Noto, V.; Tondello, E. *Electrochim. Acta* **2000**, *45*, 1211.
(7) Di Noto, V.; Barreca, D.; Furlan, C.; Armelao, L. *Polym. Adv. Technol.* **2000**, *11*, 1.
(8) Ratner, M.; Shriver, D. F. *Chem. Rev.* **1988**, *88*, 109.
(9) Ratner,M. *Polymer Electrolyte Reviews 1*; McCallum, J. R., Vincent, C. A., Eds; Elsevier Applied Science: New York, 1989; Chapter 7.
(10) Ratner, M.; Nitzan, A. *Faraday Discuss. Chem. Soc.* **1989**, *88*, 19.
(11) Druger, S. D.; Nitzan, A.; Ratner, M. *J. Chem. Phys.* **1983**, *79*, 3133.
(12) Druger, S. D.; Ratner, M.; Nitzan, A. *Phys. Rev. B* **1985**, *31*, 3939.
(13) Furukawa, T.; Imura, M.; Yuruzume, H. *Jpn. J. Appl. Phys.* **1997**, *36*, 1119.

(14) Furukawa, T.; Yoneya, K.; Takahashi, Y.; Ito, K.; Ohno, H. *Electrochim. Acta* **2000**, *45*, 1443.
(15) Ward, I. M.; Boden, N.; Cruickshank, J.; Leng, S. A. *Electrochim. Acta* **1995**, *40*, 2071.
(16) Latham, R. J.; Linford, R. G. *Solid State Ionics* **1996**, *85*, 193.
(17) Frech, R.; Chintapalli, S.; Bruce, P. G.; Vincent, C. A. *J. Chem. Soc., Chem. Commun.* **1997**, 157.
(18) Shi, J.; Vincent, C. A. *Solid State Ionics* **1993**, *60*, 11.
(19) Di Noto, V.; Longo, D.; Münchow, V. *J. Phys. Chem. B* **1999**, *103*, 2636.
(20) Lonergan, M. C.; Perram, J. W.; Ratner, M.; Shriver, D. F. *J. Chem. Phys.* **1993**, *98*, 4937.
(21) Lonergan, M. C.; Nitzan, A.; Ratner, M.; Shriver, D. F. *J. Chem. Phys.* **1995**, *103*, 3253.
(22) Roling, B.; Martiny, C.; Funke, K. *J. Non-Cryst. Solids* **1999**, *249*, 201.
(23) Roling, B. *J. Non-Cryst. Solids* **1999**, *244*, 34.
(24) Jonscher, A. K. *Dielectric Relaxations in Solids*; Chelsea Dielectrics: London, 1983.
(25) Funke, K. *Z. Phys. Chem.* **1995**, *188*, 243.
(26) Raistrick, I. D.; MacDonald, J. R.; Franceschetti, D. R. *Impedance Spectroscopy*; MacDonald, J. R., Ed.; J. Wiley & Sons: NewYork, 1987.
(27) Di Noto, V.; Lavina, S.; Longo, D.; Vidali, M. *Electrochim. Acta* **1998**, *43*, 1225.
(28) Boukamp, B. A. *Equivalent Circuit* (*EQUIVCRT.PAS*). Department of Chemical Technology, University of Twente: Enschede, The Netherlands, 1989.
(29) MacDonald, J. R.; Johnson,W. B. *Impedance Spectroscopy*; MacDonald, J. R., Ed.; J. Wiley & Sons: NewYork, 1987; p 23.
(30) Funke, K. *Ber. Bunsen-Ges. Phys. Chem.* **1991**, *95*, 955.
(31) Cramer, C.; Funke, K.; Seatkamp, T.; Wilmer, D.; Ingram, M. D. Z. *Naturforsch.* **1995**, *50a*, 613.
(32) Bunde, A.; Ingram, M. D.; Maass, P. *J. Non-Cryst. Solids* **1994**, *172*, 1222.
(33) Bishop, A. G.; MacFarlane, R. D.; Forsyth, M. *Electrochim. Acta* **1998**, *43*, 1453.
(34) Bockris, J. O'M.; Reddy, A. K. N. *Modern Electrochemistry*; Plenum: New York, 1977; Vol. 1, Chapter 4.
(35) Di Noto, V.; Bettinelli, M.; Furlani, M.; Lavina, S.; Vidali, M. *Macromol. Chem. Phys.* **1996**, *197*, 375.